



# A Real-Time Acoustic Observatory for Sperm-Whale Localization in the Eastern Mediterranean Sea

Emmanuel K. Skarsoulis<sup>1\*</sup>, George S. Piperakis<sup>1</sup>, Emmanuel Orfanakis<sup>1</sup>, Panagiotis Papadakis<sup>1</sup>, Despoina Pavlidi<sup>1</sup>, Michael A. Kalogerakis<sup>1,2</sup>, Paraskevi Alexiadou<sup>3</sup> and Alexandros Frantzis<sup>3</sup>

<sup>1</sup> Institute of Applied and Computational Mathematics, Foundation for Research and Technology - Hellas, Heraklion, Greece, <sup>2</sup> Electrical & Computer Engineering, Hellenic Mediterranean University, Heraklion, Greece, <sup>3</sup> Pelagos Cetacean Research Institute, Vouliagmeni, Greece

## OPEN ACCESS

### Edited by:

Ana Širović,  
Norwegian University of Science and  
Technology, Norway

### Reviewed by:

Natalie Posdaljian,  
University of California, San Diego,  
United States  
David Moretti,  
Naval Undersea Warfare Center  
(NUWC), United States

### \*Correspondence:

Emmanuel K. Skarsoulis  
eskars@iacm.forth.gr

### Specialty section:

This article was submitted to  
Ocean Observation,  
a section of the journal  
Frontiers in Marine Science

**Received:** 11 February 2022

**Accepted:** 11 April 2022

**Published:** 12 May 2022

### Citation:

Skarsoulis EK, Piperakis GS,  
Orfanakis E, Papadakis P, Pavlidi D,  
Kalogerakis MA, Alexiadou P and  
Frantzis A (2022) A Real-Time Acoustic  
Observatory for Sperm-Whale  
Localization in the Eastern  
Mediterranean Sea.  
*Front. Mar. Sci.* 9:873888.  
doi: 10.3389/fmars.2022.873888

A deep-water acoustic observatory for real-time detection and localization of vocalizing sperm whales was developed, deployed and operated for two 3-month periods in summer 2020 and 2021, off south-west Crete in the Eastern Mediterranean Sea, in the framework of the SAVeWhales project. Regular clicks, pulsed sounds produced by the diving animals, were detected and localized using a large-aperture array of three hydrophones suspended from surface buoys at depths of about 100 m and 1-2 km apart. Travel times of significant arrivals, arrivals with magnitude above a certain threshold, were extracted *in situ* and transmitted, together with other supporting data, via mobile broadband to a land-based analysis center. Upon reception, the data from all buoys were combined to enable detection and 3D localization of vocalizing animals exploiting direct and surface-reflected arrivals and using a Bayesian approach. The large separations between hydrophones resulted in small localization uncertainties for ranges up to 7 km; on the other hand, they posed significant challenges related to synchronization and peak association between the buoys, as well as because of the directionality of sperm whale clicks. The integrated observing system which has been successfully tested in detecting and localizing sperm whales can have a significant effect in mitigating ship strikes on whales, the prominent threat for sperm whales in the Eastern Mediterranean Sea, by providing information about the presence and location of the animals in real time. The design and implementation, as well as results from the operation and validation of the acoustic observatory are presented.

**Keywords:** sperm whales, acoustic observatory, Bayesian localization, ray theory, travel times

## 1 INTRODUCTION

Sperm whales are the largest toothed animals on the planet and have the largest brain that ever existed on earth (Marino, 2004; Roth and Dicke, 2005; McClain et al., 2015). With more than twenty deep feeding dives daily from the surface to the abyss, at depths of 1000 m or more, they are the most important link between the deep bathypelagic ecosystems and the surface waters. A single dive

has a typical duration of 40-50 min, during which the animal produces long series of pulsed sounds, so-called regular clicks, with inter-click intervals (ICIs) between 0.5 and 2 s (Goold and Jones, 1995; Jaquet et al., 2001; Amano and Yoshioka, 2003; Watwood et al., 2006). Regular sperm whale clicks are impulsive broadband signals with frequency bandwidth extending from ~300 Hz to ~30 kHz (Goold and Jones, 1995). Their high-frequency part is characterized by high directionality, whereas the low-frequency components are more omni-directional (Zimmer et al., 2005). In this connection, regular clicks have the potential both for echolocation (high directionality) and communication (omni-directionality) at the same time (Madsen et al., 2002).

The Hellenic Trench is an area in the eastern Mediterranean Sea characterized by steep bathymetry and large depths formed by the convergence between the Eurasian and African tectonic plates (Le Pichon and Angelier, 1979; Angelier et al., 1982). This area, extending from the Ionian Sea to the south of Crete and further to the sea of Rhodes, is the core habitat for the sperm whales in the Eastern Mediterranean. About 20 social units (groups of females with their juveniles and calves) of 5-15 individuals each, and at least 30 mature solitary males inhabit the Hellenic Trench (Frantzis et al., 2014). Their total number is about 200-300 and, according to all evidence, this number likely represents the total also for the entire Eastern Mediterranean Sea (Frantzis et al., 2014; Lewis et al., 2018; Frantzis et al., 2019). This is a very small and vulnerable population, yet an important piece of the European and Mediterranean wildlife. The entire Mediterranean population of sperm whales is listed as “Endangered” under the IUCN (International Union for the Conservation of Nature) Red List criteria (Notarbartolo di Sciara et al., 2006), and because of the presence of the sperm whales, the Hellenic Trench has been listed as an IMMA (Important Marine Mammal Area) at the global scale (IUCN, 2017). Ship strikes (i.e. collisions with large commercial ships) are by far the most important threat for the sperm whales of the Hellenic Trench. Major shipping lanes entering or exiting the Suez Canal and lanes connecting the Sicily Strait and the Adriatic with the Black Sea or the Eastern Mediterranean Sea, cross a large portion of the Hellenic Trench (Frantzis et al., 2019). Consequently, a heavy marine traffic area coincides with the area of the highest density of sperm whales in the eastern Mediterranean. The result is a high risk of ship strikes that are almost always fatal for the animals. Many dead sperm whales that stranded along the coasts of the Hellenic Trench during the last two decades bear propeller marks and injuries that have been provoked by ship strikes (Frantzis et al., 2019).

To address the problem of ship strikes, a system for real-time detection and localization of sperm whales from their clicks was designed in the framework of the SAWEWhales project (System for the Avoidance of Ship-Strikes with Endangered Whales). A pilot version of this system was developed, deployed and operated for two 3-month periods in summer 2020 and 2021 off south-west (SW) Crete, specifically in the periods from 1 July to 2 October 2020 and from 26 May to 3 September 2021. Detection and localization was based on clicks arriving over direct and surface-reflected paths at a large-aperture array of

three hydrophones suspended from surface buoys at depths of about 100 m and 1-2 km apart from one another. Travel times of significant arrivals were extracted *in situ* and transmitted, together with other supporting data, *via* mobile broadband to a land-based analysis center where the data from all buoys were combined to enable detection and 3-dimensional (3D) localization of vocalizing animals in real time. The system performance was assessed by means of two verification campaigns and a controlled localization experiment.

Various setups have been proposed in the literature for localization of pulsed sources, ranging from two hydrophones (Watkins and Schevill, 1972; Hastie et al., 2003) and multi-hydrophone towed linear arrays (Teloni, 2005; Tran et al., 2014) to more complicated 3D arrays of various geometries (Wahlberg et al., 2001; Rideout et al., 2013). The most common localization approach is through intersection of hyperboloids corresponding to the time differences of arrival (TDOAs) between arrivals at the different hydrophone pairs (Morrissey et al., 2006; Miller and Dawson, 2009; Baggenstoss, 2011; Miller et al., 2013; Brunoldi et al., 2016), which can be regarded as a generalization of methods for bearing estimation (Watkins and Schevill, 1972; Leaper et al., 1992). Networks of asynchronous compact tetrahedral arrays have also been proposed, allowing for 3D localization through triangulation or back propagation (Urazghildiiev and Hannay, 2017; Urazghildiiev and Hannay, 2020; Sanguineti et al., 2021). Networks of asynchronous free-drifting acoustic stations with suspended hydrophone pairs have been applied for localization and animal density estimation (Barlow et al., 2018; Barlow et al., 2021), whereas combinations of different receiving stations of various types, such as single hydrophones, vertical line arrays and compact hydrophone arrays have also been used (Gassmann et al., 2013; Gassmann et al., 2015).

3D localization based on direct and surface-reflected arrivals was originally introduced in connection with receptions at two hydrophones separated in the horizontal, e.g. two-hydrophone towed arrays, first assuming homogeneous environments (Skarsoulis et al., 2004; Thode, 2004) and then generalizing for refractive environments using ray-theoretic approaches (Skarsoulis and Kalogerakis, 2005; Thode, 2005; Skarsoulis and Kalogerakis, 2006; Skarsoulis and Dosso, 2015). In those approaches source range and depth estimation only requires knowledge of hydrophone depths, not their location in the horizontal; if the latter is also known, then the source azimuth can be estimated too. This method was tested in the field, in a series of controlled localization experiments as well as for the localization of sperm whales using large-aperture towed two-hydrophone arrays (Thode, 2004; Thode, 2005; Skarsoulis et al., 2018). Two-hydrophone localization is subject to left-right ambiguity, and localization uncertainties are subject to angular dependence. Source locations close to the endfire result in large azimuth uncertainties, while source locations close to the broadside result in large range and depth uncertainties (Skarsoulis and Dosso, 2015; Skarsoulis et al., 2018). Those pitfalls can be addressed by adding a third hydrophone, not in line with the other two (Pavlidis and Skarsoulis, 2021). Thus, a three-hydrophone configuration results in a more uniform coverage with respect to the azimuth concerning

localization uncertainties, and provides useful fallback options in case one of the hydrophones drops out. Since fault tolerance and enhanced coverage/accuracy are of critical importance for long-term operational networks, this last approach was adopted for the SAvEWales observatory, which was designed and implemented as a three-hydrophone system.

The contents of this work are organized as follows: In Section 2 the main components of the SAvEWales system are briefly described. These include the acoustic stations and their on-board processing – wet end – and the detection and localization algorithms at the analysis center – dry end of the system. Section 3 describes the deployment of the acoustic system and the verification campaigns, as well as a controlled localization experiment conducted in August 2021. Intermediate and final localization results as well as comparison of the latter with independent observations from the verification campaigns are presented in Section 4, along with the results from a controlled localization experiment. Finally, a discussion of basic results and possible future developments is given in Section 5.

## 2 THE SaveWhales DETECTION AND LOCALIZATION SYSTEM

A system for the mitigation of ship strikes requires real-time detection and localization on a 24/7 basis. Taking into account that ICIs of regular sperm-whale clicks typically range from 0.5 to 2 s, and that there may be more than one vocalizing animals at the same time, e.g. in the case of social units, the processing and localization analysis has to be fast enough to keep up with the incoming data.

The SAvEWales detection and localization system consists of three moored acoustic stations, each equipped with a hydrophone, which record click sounds, process them and transmit processing results to the analysis center based at FORTH (Foundation for Research and Technology – Hellas) in Heraklion, where the information from all three stations is gathered and combined to perform sperm-whale detection and localization.

### 2.1 The Acoustic Stations

The SAvEWales Acoustic Network (SWAN) consists of three moored acoustic stations, nicknamed SWAN1, SWAN2, SWAN3 (or in abbreviated form S1, S2 and S3, respectively). Each station consists of a surface buoy equipped with a self-contained solar-powered autonomous communication and processing system connected to a hydrophone at 100-m depth. Further, it is equipped with a GPS receiver to provide location data and has two-way communication with the analysis center at FORTH. Pulse-per-second (PPS) signals emitted from the GPS satellites are used for high-accuracy time synchronization among the stations. The buoy is assembled around a custom-made stainless steel skeleton with floaters attached on the upper part and a base at the underwater lower part to accommodate the battery of the system.

The components of each acoustic station are as follows (see also **Figure 1**): A high-sensitivity, broadband (up to 60 kHz), low-noise hydrophone (Benthowave Instruments Inc. model BII-7121) along with a depth and temperature sensor (STS ATM.1ST/T - High Precision Transmitter) are accommodated in a waterproof cylindrical canister, which can sustain water pressure at depths up to 200 m. The hydrophone canister is connected to a MacArtney 100-m long power and data cable (MacArtney 4588 4 STP) through a SubConn socket enabling easy replacement and servicing. The other end of the cable is plugged into the so called “CPU box” above the surface, an IP67 watertight casing where all the electronics are accommodated. The central processing unit is a Raspberry Pi 2 single-board computer which controls the GPS/PPS, communication and data acquisition modules, performs data processing, data telemetry of extracted information as well as storage of raw data. The data acquisition unit is a USB-1608FS-Plus by MCC with eight single-ended analog channels, 16-bit resolution and up to 100 kSamples/s sampling rate per channel; it is used for simultaneous recording of acoustic and PPS data, as well as for acquisition of auxiliary data from depth and temperature sensors, battery voltage etc. For the reception of GPS and PPS data, a Raspberry card by Adafruit (Ultimate GPS hat for Raspberry Pi) is used. Data telemetry, two-way communication



**FIGURE 1** | The SWAN acoustic station (from left to right): Hydrophone canister with Benthowave hydrophone and STS depth/temperature sensor, power/data cable, battery, floats, CPU box, solar panel plate.

and remote control is carried out through a Raspberry card by Sixfab (4G/LTE Cellular Modem Kit for Raspberry Pi). Finally a Western Digital 1-TB SSD unit is used for storage of raw data. Each station is powered through a solar power system consisting of a 12 V/60 W/55×68 cm<sup>2</sup> semi flexible solar panel at the top of the buoy, a regulator by EPEVER (model XTRA2210N) inside the CPU box and a 12 V/80 Ah deep-cycle battery encased in 1-cm thick polyester mold accommodated at the bottom end of the buoy (~2 m below the sea surface) and connected to the CPU box through a MacArtney 6589 cable. The battery is placed there to also serve as ballast weight and increase flotation stability.

The recording and processing routine for each acoustic station consists in recording sound with a sampling frequency of 100 kHz for a period of 1 minute (60 s) every 3 minutes. The duty cycle is fully parametrized; the particular one was decided taking into account energy constraints and also considering that for a typical dive duration of 45 minutes there will be a sufficient number (~15) of 1-minute recordings. Further, for ICIs typically between 0.5 and 2 s, a 1-minute recording is expected to include a large number of clicks to allow for several localizations of a vocalizing whale, while the distance of an animal moving at an average speed of 1-2 knots (Watkins et al., 1993) will not change much (30-60 m) in the course of 1 minute. The 2-minute interval between subsequent recordings gives enough time for onboard processing and data telemetry, whereas it keeps power consumption and data storage requirements within limits.

The acoustic recordings are processed in situ: they are bandpass filtered between 1 and 20 kHz with a 50-dB convolution filter and then they are energy-filtered by applying a 1-ms sliding window to reveal acoustic peaks. A subset of these peaks is selected by applying a time-variable threshold to account for changing noise conditions. The threshold is set to the 4-fold of the background noise level, estimated as the mean output of the energy filter, in every 1-s interval.

The PPS time series is digitized simultaneously with the acoustic time series, with the same sampling frequency (100 kHz), to provide a reference for synchronization. The PPS signal is a 100-ms box-shaped pulse with 1-s repetition period emitted from the GPS satellites. Every SWAN buoy processes each 1-minute PPS recording to isolate the pulse signals and estimate their arrival times to be used as synchronization reference.

The times and amplitudes of the selected acoustic peaks together with the synchronization data and other state variables (hydrophone depth, battery voltage, etc.) are transmitted to the analysis center a few seconds after completion of the onboard processing, whereas the raw data – original recorded time series – are internally stored for post-recovery detailed analysis.

## 2.2 Processing at the Analysis Center

Data from the three SWAN buoys arrive at the analysis center at FORTH on a regular basis, every 3 minutes. These data consist primarily of the times and amplitudes of significant acoustic arrivals (selected peaks) from the 1-minute recording at each acoustic station, as well as other auxiliary data including mooring GPS locations, hydrophone depths, time synchronization data, and more. Once received, the data from the three acoustic

stations are combined and streamed through a multistage analysis system to produce detection and localization results. The main stages of this process are briefly presented below.

*Detection of Regular Click Trains:* The incoming acoustic data contain arrivals from many sources of pulsed sounds (snapping shrimp, dolphins, ships, etc.), other than sperm whales. To detect regular sperm-whale clicks, the received arrival train from each hydrophone is searched for the existence of regular arrival patterns, i.e. repeating arrivals with constant or slowly varying repetition period within the typical ICI range for regular sperm-whale clicks, from 0.5 to 2 s. The detection algorithm focuses on the peaks of the histogram of arrival-time differences at each hydrophone to reveal dominant separations within the above range. If the corresponding arrival times exhibit regularity, within some tolerance, which is associated with the discretization of the time histogram, typically set to 0.2 s, and their number exceeds a minimum value, a detection flag for the particular hydrophone is raised.

A “detection event” is confirmed either i) when there are at least two detection flags raised in the current 1-minute recording (detection at two different hydrophones) or ii) when there is one detection flag raised in the current 1-minute recording and at least one more detection flag raised in any of the previous two 1-minute recordings. The above scheme was decided in an effort to increase the statistical significance of the detections and reduce the probability of false alarms, taking into account that sperm whale clicks can sometimes be confused with ship noise. Further, due to the large separation between the hydrophones and the directionality of sperm whale clicks, the latter may be received and detected at only one hydrophone, which may be different in subsequent 1-minute recordings. **Figure 2** presents a typical case of sperm-whale detection at the three hydrophones in a 1-minute recording.

Following the detection of regular click patterns, the arrival-time data are further processed and subjected to localization analysis. This includes the following steps: a) time synchronization using PPS reference data, b) search for pairs of direct and surface-reflected arrivals to be preserved, c) initial data scan and bearing estimation, d) arrival association between hydrophones, e) source range/depth estimation, and finally f) azimuth estimation based on receptions at three or two hydrophones. A description of each processing step is given below, and typical processing results (intermediate results) are presented in Section 4.1.

(a) *PPS Correction:* The received synchronization data, i.e. the arrival times of the PPS pulses at each acoustic station, are processed to estimate the relative delays for the three hydrophone pairs (SWAN1-SWAN2, SWAN1-SWAN3, SWAN2-SWAN3). These delays are then used to bring the corresponding three sequences of acoustic arrival times to a common time reference. Prior to the PPS correction the acoustic time series are synchronized within a few milliseconds. After the PPS correction a synchronization accuracy of the order of 1 microsecond is achieved.

(b) *Arrival Pairing:* Since the targeted source localization relies on TDOAs between pairs of direct and surface-reflected arrivals at each hydrophone, it is important to identify such pairs

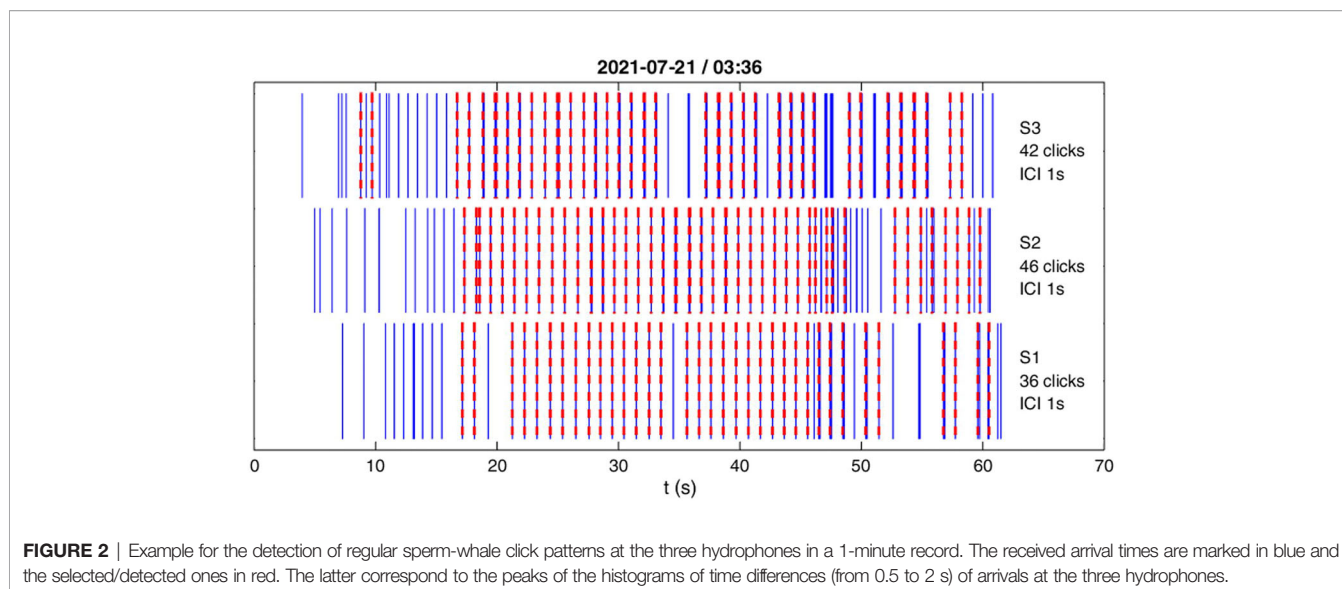


**FIGURE 2** | Example for the detection of regular sperm-whale click patterns at the three hydrophones in a 1-minute record. The received arrival times are marked in blue and the selected/detected ones in red. The latter correspond to the peaks of the histograms of time differences (from 0.5 to 2 s) of arrivals at the three hydrophones.

early on and tag them together, in order to preserve them against splitting and erroneous associations. Such arrival pairs are identified by exploiting the fact that the time difference between direct and surface-reflected arrivals (TDOA) at the receiver depends on the source location, and thus for an animal at a distance of several km it is not expected to change much in the course of the 1-minute recording, taking into account typical average sperm whale speeds of 1–2 kn at foraging depths (Watkins et al., 1993). Thus, in a reception containing a regular click train, the corresponding TDOA will stand out as a sharp peak in the histogram of arrival time differences.

*(c) Initial Source Location Scan:* This step provides an initial estimation of the source bearing by scanning the candidate source locations in the horizontal plane. For each location the corresponding time offsets at the different hydrophones are estimated assuming constant sound speed (1500 m/s) and ignoring the difference in depth between the source and the hydrophones. The estimated offsets are subtracted from the corresponding arrival times which are then compared for matches. The number of arrival matches (the sum of matches over all hydrophone pairs) is a measure of likelihood of the particular source location, and its spatial distribution reveals the dominant azimuthal direction(s). Thus, a first approximation for the source bearing(s) can be obtained.

*(d) Arrival Association:* The correct association of arrival times between the different hydrophones is crucial for 3D localization. This association is challenging because of the large separation between hydrophones, which may cause relative delays in the arrivals up to 1 s, depending on the location of the source. Since the ICI values typically range from 0.5 to 2 s, it may occur that a click arrives at the hydrophone closest to the animal before the previous click has arrived at a distant hydrophone, due to which the association between peaks at the different hydrophones is far from straightforward. The association problem is addressed here by first applying a pattern cross-correlation method looking for similarities

in the available arrival trains (Park et al., 2008). The resulting cross-correlation offsets are then checked for geometric compatibility, i.e. it is examined whether there exist candidate source locations resulting in similar time offsets. If there exist such locations, then the offsets resulting from the cross-correlation procedure are subtracted from the arrival times to align corresponding peaks and make associations.

*(e) Source Range/Depth Estimation:* The source ranges (horizontal distances from the hydrophones) and source depth, together with their respective uncertainties are estimated by applying a Bayesian iterative localization scheme (Skarsoulis and Dosso, 2015; Pavlidi and Skarsoulis, 2021). Depending on the arrival associations obtained in the previous step, whether between all three hydrophones or between two hydrophones only, the corresponding three-hydrophone (3H) or two-hydrophone (2H) localization scheme is applied, respectively. It is worth noting that this step requires knowledge of hydrophone depths only, not of their location in the horizontal; this is because the information about the relative ranges is contained in the TDOAs between the direct arrivals.

*(f) Source Localization in the Horizontal:* The source ranges estimated in the previous step are combined with the hydrophone locations in the horizontal, estimated from the GPS fixes and taking into account the hydrophone depths, to obtain the source location in the horizontal as well (Skarsoulis and Dosso, 2015; Pavlidi and Skarsoulis, 2021). In the case where the localization is based on two hydrophones, there are two geometrically symmetric solutions, symmetric with respect to the line connecting the two hydrophones in the horizontal plane (left-right ambiguity); if one of the two falls in a shallow-water area or on land, it is ignored.

At the analysis center, the above processing and analysis steps are executed automatically on a routine basis in real time for each acoustic recording received. Special care is taken for the algorithms to be fast enough to keep up with the incoming data flow. For this purpose the localization codes are implemented using efficient

programming in C resulting in short execution times, typically less than 0.03 s per localization, while the overall processing time for a 1-minute recording is typically less than 10 seconds. This is crucial for the development of a real-time monitoring system, taking into account that regular sperm whale clicks have ICIs typically between 0.5 and 2 s, which means that there may be a need for several localizations per second, especially in the case of social units and multiple vocalizing animals.

### 3 FIELD OPERATIONS

The deployments of the SAvEWhales observatory in 2020 and 2021, as well as the efforts for the assessment of the localization performance, namely the verification campaigns and the controlled localization experiment, are described in the following.

#### 3.1 Deployment of the Observatory

The SAvEWhales observatory was deployed and operated for two 3-month periods, in summer 2020 and 2021, in the Bay of Sougia off SW Crete (see **Figure 3**), at water depths between 450 and 550 m. The buoys, with 1–2 km separation from each other, formed an obtuse triangle with its longest side roughly aligned with the 500-m isobath. The first deployment period was from 1 July to 2 October 2020 and the second one from 26 May to 3 September 2021.

The deployments were carried out using the fishing vessel FV ELENA. They were quite demanding due to the large water depths and bottom slopes (slope angles reaching or exceeding 20°). Each buoy was kept in place by two anchors, deployed north and south of its target location and attached with chains to the anchor lines, ropes of lengths 600 m and 700 m, respectively. Thus, the anchor lines formed a capital-lambda ( $\Lambda$ ) shape allowing the buoy some freedom for movement in the east-west direction (parallel to the isobaths), the primary direction of the prevailing currents in the area, and leaving free space for the hydrophone cable in the middle.

Towards the end of the first deployment, in September 2020, a strong hurricane hit western Crete, and in its aftermath on 22

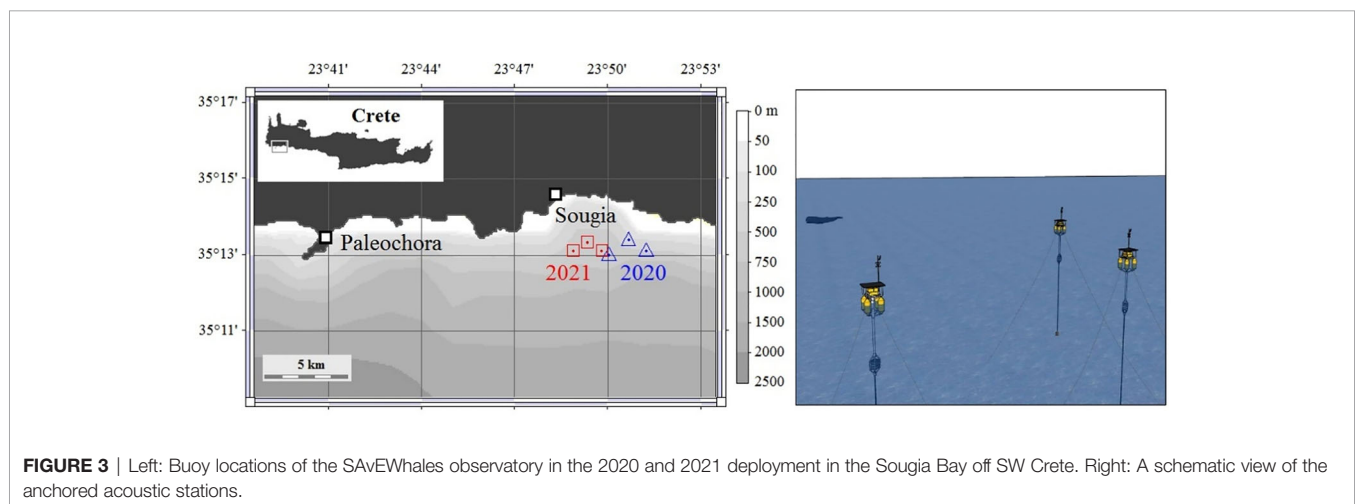
September an extremely strong W-NW current set in and sank the east and west buoys, SWAN2 and SWAN3. Following this loss, two new buoys were constructed for next year's deployment, and all three buoys were secured with extra floaters providing additional excess buoyancy. Further, in the 2020 deployment the central and especially the east hydrophone received a lot of noise from snapping shrimp. In an effort to obtain better ambient noise conditions, the mooring locations in 2021 were displaced by about 2 km to the west, compared to the 2020 locations (see **Figure 3**). The noise conditions were indeed much better in the 2021 deployment, however this was at the cost of increased weather exposure of the instruments as they came closer to the axis of the Sougia channel, a passage between mountains in the Sougia area, giving rise to strong north wind gusts.

During the two deployment periods the deployment site was visited regularly, nearly every two weeks, for instrument inspection and maintenance. At each visit the temperature profile in the water column was measured using a temperature-depth recorder (RBR TDR-2050 and RBRduo) to get updated estimates of the sound-speed profile affecting refraction and accounted for in the localization process. The corresponding sound-speed profiles were calculated using the Chen-Millero formula (Chen and Millero, 1977) assuming a constant salinity value of 39 ppt which is typical for the Eastern Mediterranean Sea (Grodsky et al., 2019).

A significant number of sperm-whale detections were performed by the SAvEWhales system, nevertheless there was a significant difference in the detections registered during its two deployment periods in 2020 and 2021: Sperm whales were detected on only 4 days in 2020, compared to 42 detection days in 2021. The detection hours per day are presented in **Figure 4**, and it is seen that not only the detection days are fewer in 2020 but also the daily duration of detection: in 2020 there is only one day with more than 2 hours of detection whereas in 2021 there are several days with more than 6 detection hours.

#### 3.2 Verification Campaigns

Over the course of the deployment periods two verification campaigns were conducted in the broader area of the



deployment site, the first between 20 July and 11 August 2020 and the second between 16 and 29 July 2021, using a sailing vessel, to provide independent observations as ground for comparisons and validation of system performance.

During the first verification campaign there were no encounters with sperm whales at all in the broader area of SW Crete. This is consistent with the fact that the very few detections registered by the SAvEWhales system during the 2020 deployment were outside the period of the verification campaign (**Figure 4A**). In contrast, in the 2021 deployment, there were several sperm-whale detections during the verification campaign, which also provided sufficient data (resolved direct and surface-reflected arrivals) for 3D localizations such that comparisons could be carried out. These comparisons are presented in section 4.1.

In both verification campaigns acoustic observations were obtained using a small-aperture array of two hydrophones with 3-m spacing towed behind the vessel with the cable of 100 m. This configuration allows for bearing estimation exploiting TDOAs between direct arrivals. In this connection verifications focused mostly on instances where the vocalizing animals were close to the broadside (abeam) of the array, i.e. in a direction perpendicular to the course of the vessel, which is also the direction associated with the smallest uncertainties in azimuth estimation. The left-right ambiguity of bearing estimation induced by this setup was resolved either through appropriate maneuvering of the vessel (change of course direction) or from visual observations of the animal when at the surface.

### 3.3 Controlled Localization Experiment

On 27 August 2021 between 7:00 and 11:00 a controlled localization experiment was conducted to assess the localization performance of the SAvEWhales observatory. The experiment involved the deployment of a pinger from FV Elena

at various ranges (2, 4 and 6 km from the central acoustic station SWAN1) and depths up to 850 m and comparisons between the localization results and the actual pinger location. An ONLINE-1260 pinger emitting 4-ms pulses of central frequency 10 kHz with repetition period 17 s and source level 190 dB re 1  $\mu$ Pa @ 1 m was used. A RBR-Duo temperature-depth recorder was attached to the pinger (**Figure 5A**) to provide data about the actual depth. At each station the vessel turned off its engine and GPS fixes were taken.

The sea surface on the particular day was rather rough corresponding to sea state 3-4 (**Figure 5B**) which contributed to increased wander of surface-reflected arrivals. The sound-speed profile resulting from the temperature profile measured on that day corresponds to typical late-summer conditions, with sound-speed increase towards the surface in the upper 150-m layer and a sound-speed minimum at the depth of 170 m followed by a weak sound-speed increase up to about 700 m and then a moderate increase at larger depths (**Figure 5C**).

## 4 LOCALIZATION RESULTS

This section presents localization results from the SAvEWhales observatory and comparisons with independent observations obtained during the 2021 verification campaign and a controlled localization experiment.

### 4.1 Comparisons with Observations from the 2021 Verification Campaign

As already mentioned, the acoustic observations during the two verification campaigns were obtained using a towed small-aperture array of two hydrophones. **Table 1** contains the vessel

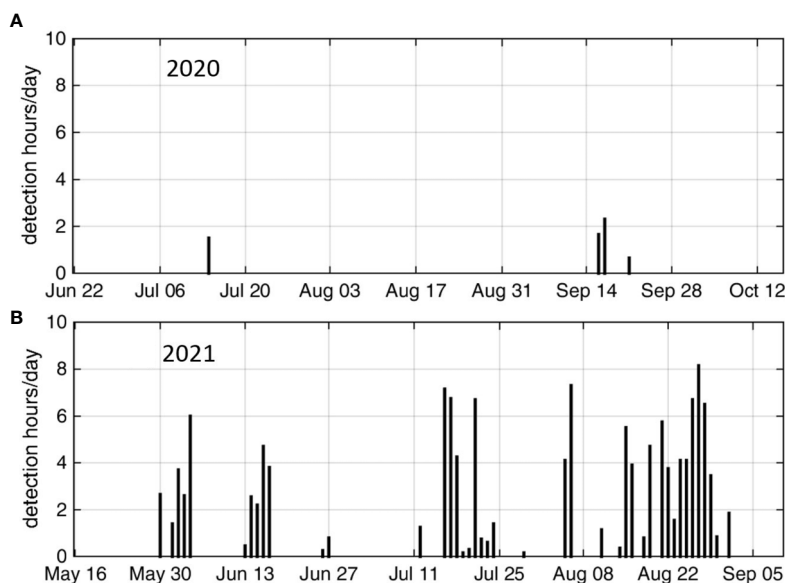


**FIGURE 4** | Daily sperm-whale detections during the deployments **(A)** in 2020 and **(B)** in 2021.

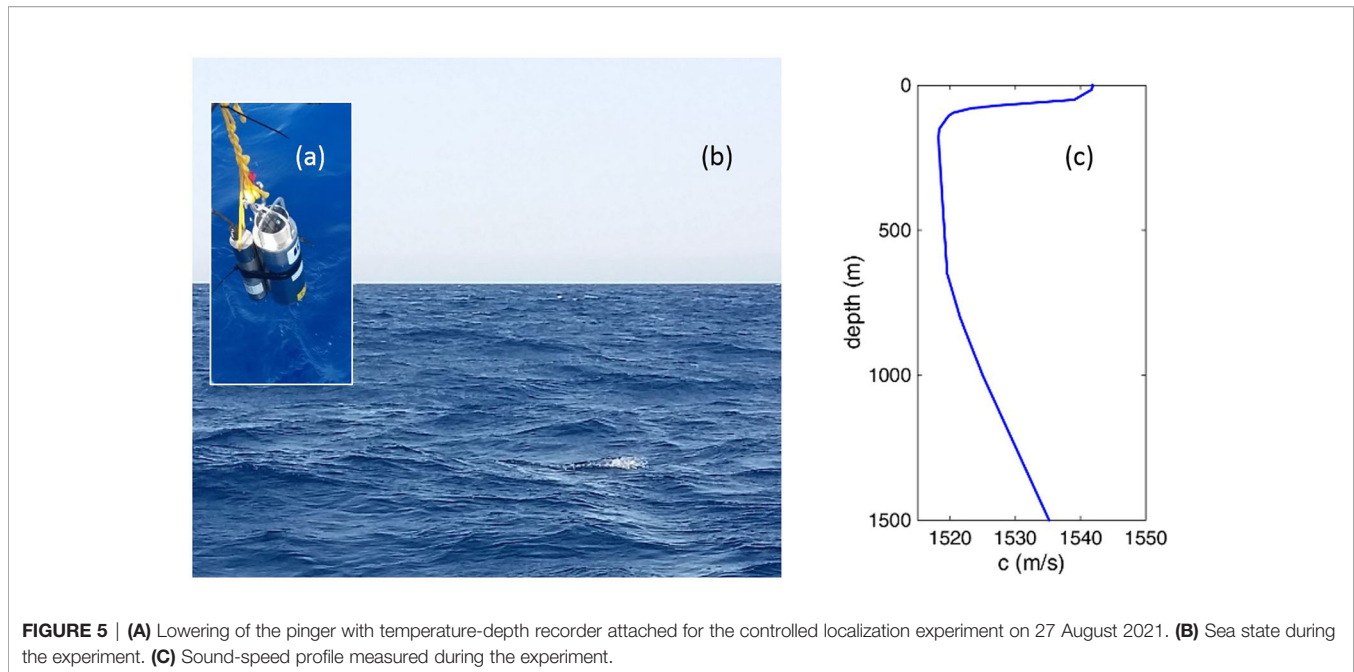


**FIGURE 5 | (A)** Lowering of the pinger with temperature-depth recorder attached for the controlled localization experiment on 27 August 2021. **(B)** Sea state during the experiment. **(C)** Sound-speed profile measured during the experiment.

position and heading at the time of three acoustic observations (termed as cases “A”, “B” and “C”) during the 2021 verification campaign to be compared against SAvEWhales localizations. In case “A” the intermediate results from the localization analysis are also presented, in Figs. 6-9, to demonstrate the processing chain behind each localization. Although visual observations of sperm whales at the surface were also conducted by the vessel’s crew, there were no simultaneous localization results to compare with, since acoustic localization applies to vocalizing animals during deep dives but not while at surface, where they do not produce regular clicks.

#### 4.1.1 Case “A” (16 July 2021 16:02:35)

The acoustic recording nearest to the observation time is the one starting at 16:03. The arrival patterns at the three hydrophones from that recording after synchronization are shown in **Figure 6**. The labels S1, S2 and S3 correspond to SWAN1, SWAN2 and SWAN3, the central, west and east hydrophone, respectively. Due to the presence of noise regular click trains are indistinguishable at this point in the analysis process.

*Arrival Pairing:* The histograms of time differences between arrivals at each of the three hydrophones are shown in the upper

three panels of **Figure 7**, respectively, revealing that there is a concentration about 15 ms for SWAN1, 23-25 ms for SWAN2 and 13.5 ms for SWAN3. These concentrations suggest that there are repeated clicks from a sound source at a particular location with resolved direct and surface-reflected arrivals separated by the above time values. Since the TDOA between direct and surface-reflected arrivals of a source at a particular depth decreases with range, the above numbers indicate that the source is closest to SWAN2, further from SWAN1 and even further from SWAN3. The bottom panel in **Figure 7** shows the arrival pairs, i.e. pairs of direct and surface-reflected arrivals, corresponding to the peaks of the histograms above; the temporal separation in each pair is smaller than 30 ms, so the pairs cannot be visually resolved in this figure. This is a subset of the arrivals shown in **Figure 6** and exhibits a clear regularity, typical for sperm-whale click trains. Once identified, the arrival pairs are locked together and preserved throughout the subsequent analysis.

*Initial Source Location Scan:* Using the paired arrivals an initial scan of candidate source locations can be performed to obtain a first estimate of the source azimuth and possibly a first very rough estimate of the source range. As already mentioned,

**TABLE 1 |** Vessel position and heading at the time of three acoustic observations using a towed two-hydrophone array during the 2021 verification campaign.

	Date 2021	Local time	Vessel Position	Vessel Heading	Remarks
A	16 July	16:02:35	35°12.737'N 23°48.035'E	285.8°	Whale abeam at portside
B	16 July	16:12:41	35°11.848'N 23°47.868'E	188.6°	Whale abeam and close to the boat (few hundred meters, as inferred from visually observed surfacing shortly after)
C	21 July	17:25	35°11.537'N 23°47.306'E	263.4°	Whale abeam and very close to the boat (few tens meters, as inferred from visually observed fluking shortly before)

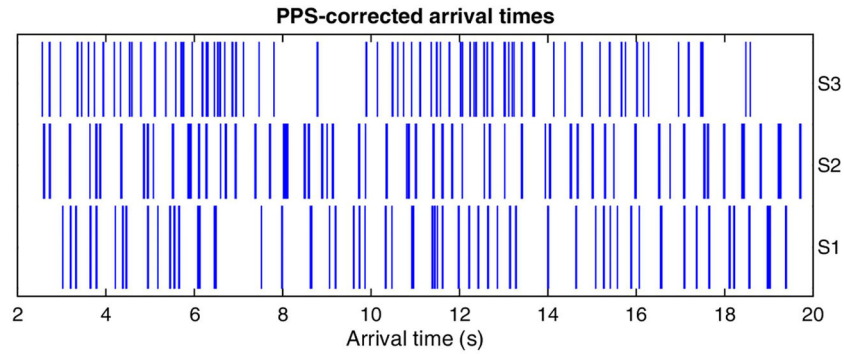


**FIGURE 6** | Arrival patterns on 16 July 2021, at 16:03 after synchronization (PPS correction) of the recordings at the three hydrophones SWAN1, SWAN2 and SWAN3.

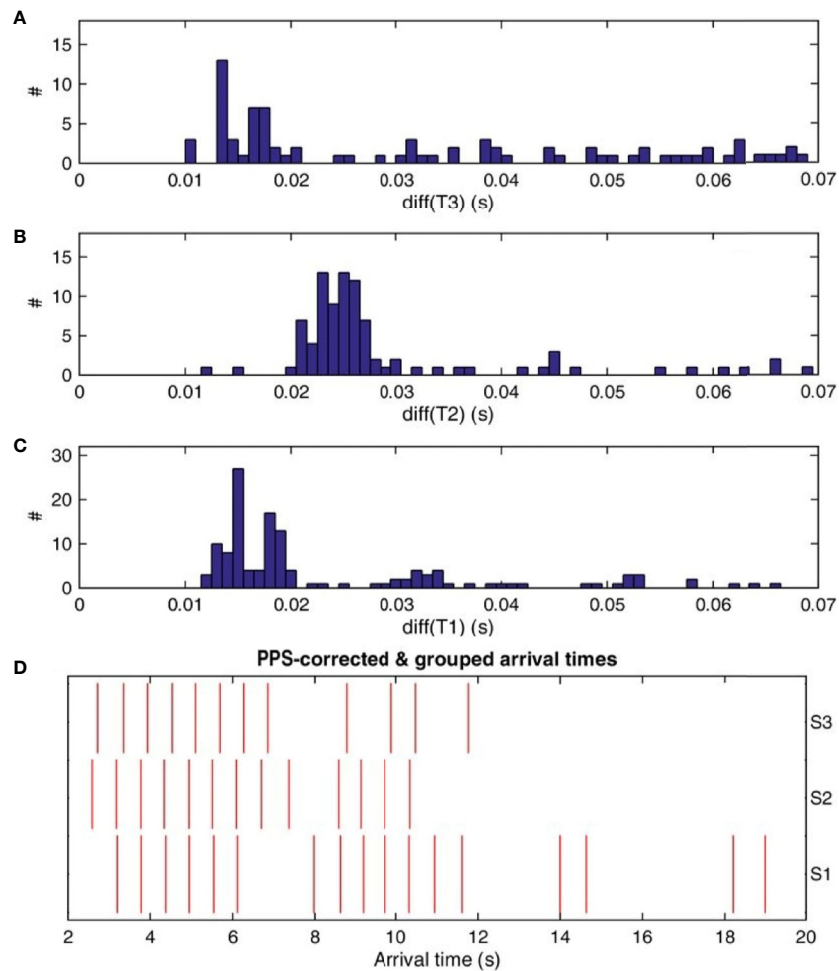


**FIGURE 7** | Histograms of time differences (up to 70 ms) of arrivals recorded at **(A)** SWAN3, **(B)** SWAN2 and **(C)** SWAN1 and shown in **Figure 6**; the vertical axes (#) in panels **(A–C)** measure histogram counts. **(D)** Pairs of direct and surface-reflected arrivals corresponding to the histogram peaks in **(A–C)** – a subset of those shown in **Figure 6**.

for each candidate source location the corresponding time offsets at the different hydrophones are estimated assuming constant sound speed (1500 m/s) and ignoring the difference in depth between the source and the hydrophones. The estimated offsets are subtracted from the corresponding arrival times, which are then compared for matches. Thus, for each candidate location, a number of matches is calculated, which can be used as a measure of the likelihood of a particular location. The distribution of the number of matches as a function of the source location is shown in **Figure 8**. The highest values (in red) are observed along a line at the southwest of the SAveWhales array – the SWAN stations are marked by the black dots in this figure – at distances between 2.5 and 4 km from the central station SWAN1. These are very preliminary estimates to be replaced by improved 3D localization results in the following. Nevertheless, these estimates can be useful in cases where 3D localization results are not available (e.g. due to a failure in arrival association or divergence of the range/depth estimation algorithm).

**Arrival Association:** The full 3D localization relies on the TDOAs between direct and surface-reflected arrivals at each hydrophone, as well as TDOAs between direct arrivals at the different hydrophones. The latter require the arrivals at the different hydrophones to be associated with each other. This problem is addressed by first applying a pattern cross-correlation method (Park et al., 2008) looking for similarities and possible offsets in the available arrival trains. The resulting offsets are then examined for compatibility with the geometry, in the sense that there exists at least one candidate source location resulting in similar time offsets.

The cross-correlation histograms between the arrival times for the three hydrophone combinations, T3-T2, T3-T1 and T2-T1 are shown in the upper three panels of **Figure 9**. The offsets corresponding to the histogram peaks are compatible with each other – they sum up to zero – and they are also compatible with the geometry, i.e. there exist source locations resulting in comparable offsets. By applying the opposites of the T3-T1 and T2-T1 offsets to the arrival patterns at SWAN3 and SWAN2, respectively, the peaks

in the shifted arrival patterns become aligned with those in the arrival pattern at SWAN1, which allows for direct arrival matches. This can be seen in the bottom panel of **Figure 9** presenting 14 peak associations, marked by the black dashed lines, of which 8 between all three hydrophones, 3 between SWAN1 and SWAN2, 2 between SWAN1 and SWAN3, and finally 1 between SWAN2 and SWAN3. Using these associations, the TDOAs required for the 3D localization can be estimated.

**Localization:** With the pairs of direct and surface-reflected arrivals at each hydrophone identified (**Figure 7**) and the direct arrivals at the different hydrophones associated (**Figure 9**) the corresponding TDOAs can be calculated and the 3D localization carried out. The localization results are shown in **Figure 10**. The top panel in that figure shows in orange color the localization results in the horizontal and the corresponding root-mean-square uncertainties (RMS ellipses) based on all three hydrophones (3H localizations), i.e. corresponding to the 8 arrival associations between the three hydrophones shown in **Figure 9D**. It is seen that all localizations are at about 3.6 km to the S-SW of the central acoustic station SWAN1, and all are in agreement with each other. The straight line segments mark the position and direction of the verification cruise vessel: the blue line and the small open circle display the course and the location of the vessel at 16:02:35, the time of the observation, whereas the broadside direction is represented by the black line, 100 m behind the boat and perpendicular to its course. It is seen that the SAveWhales localization is very close to this line at a distance of about 1 km from the vessel course.

The embedded graph in **Figure 10A** shows the sound-speed profile resulting from temperature measurements in mid July, which is taken into account for the localization. This profile corresponds to typical mid-summer conditions, with a sound-speed increase towards the surface in the upper 100 m, a sound-speed minimum at 170-m depth and sound-speed increase at larger depths. The temperature profiles measured from late spring till early autumn in 2020 and 2021 in the area all exhibited shallow seasonal thermoclines giving rise to a sound-

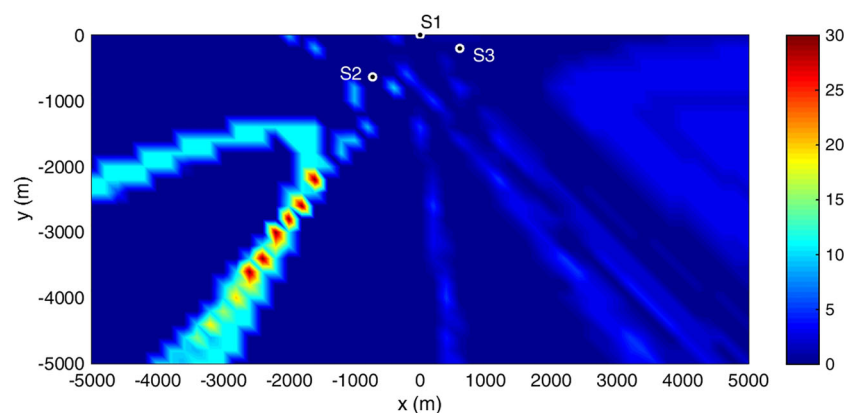


**FIGURE 8** | Initial search for source location in the horizontal based on associations between paired arrivals at the different hydrophones, those shown in **Figure 7D**. The three black dots indicate the mooring locations and the color represents the association count as a function of source location.

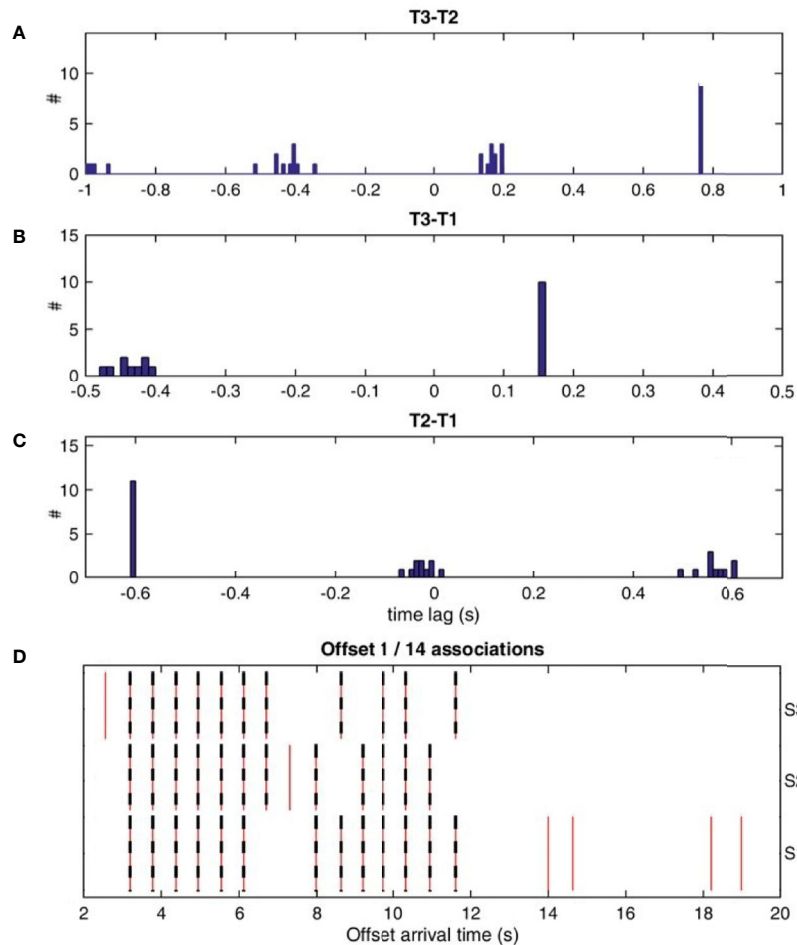


**FIGURE 9** | Cross-correlation histograms between the arrival patterns of **Figure 7D** for the three different hydrophone combinations: **(A)** SWAN3-SWAN2, **(B)** SWAN3-SWAN1 and **(C)** SWAN2-SWAN1; the vertical axes (#) in panels **(A–C)** measure histogram counts.. **(D)** Aligned arrival patterns (red) using the opposites of the offsets in panels **(B, C)**. Arrival associations (14 in total) are marked by the black dashed lines; 8 of them correspond to arrival associations among all three hydrophones (enabling 3H localizations) while the rest 6 correspond to arrival associations between various pairs of hydrophones (enabling 2H localizations).

speed minimum at about 170-m depth, with the main differences concentrated in the surface layer: increasing sound speed at the surface and increasing depth of the surface layer in the course of the summer, as can be seen by comparing the sound-speed profiles in Figs. 10 and 5. The use of the correct profile is important for an accurate localization, since acoustic refraction has a significant effect on localization performance (Skarsoulis and Dosso, 2015). Ray diagrams and effects of refraction on localization performance for typical conditions in the particular area can be found in previous works (Skarsoulis and Dosso, 2015; Skarsoulis et al., 2018; Pavlidi and Skarsoulis, 2021).

2H localization results in the horizontal from various combinations of two hydrophones are shown in red color in the middle panel of **Figure 10**, corresponding to the 6 associations between two hydrophones in **Figure 9D**. In order to interpret these localization results one has to recall that 3D localizations based on two hydrophones are characterized by large range and depth uncertainties for sources in the broadside

direction, decreasing towards the endfire, and by large azimuth uncertainties for sources in the endfire direction, decreasing towards the broadside (Skarsoulis and Dosso, 2015). Two of the localizations in **Figure 10B** have large range and small azimuth uncertainties, whereas the other four have small range and larger azimuth uncertainties. The former correspond to the associated arrivals between SWAN1 and SWAN3 (2 associations in **Figure 9D**), which have the source close to their broadside in the horizontal plane. This results in large range and small azimuth uncertainties. The other four localizations correspond to associations between SWAN1 and SWAN2 (3 associations), and also between SWAN2 and SWAN3 (1 association) in **Figure 9D**. Both pairs (SWAN1-SWAN2 and SWAN2-SWAN3) have the source close to their endfire in the horizontal plane, and this results in small range uncertainties and larger azimuth uncertainties.

2H localizations are subject to left-right ambiguity in the horizontal resulting in symmetric location estimates about the line

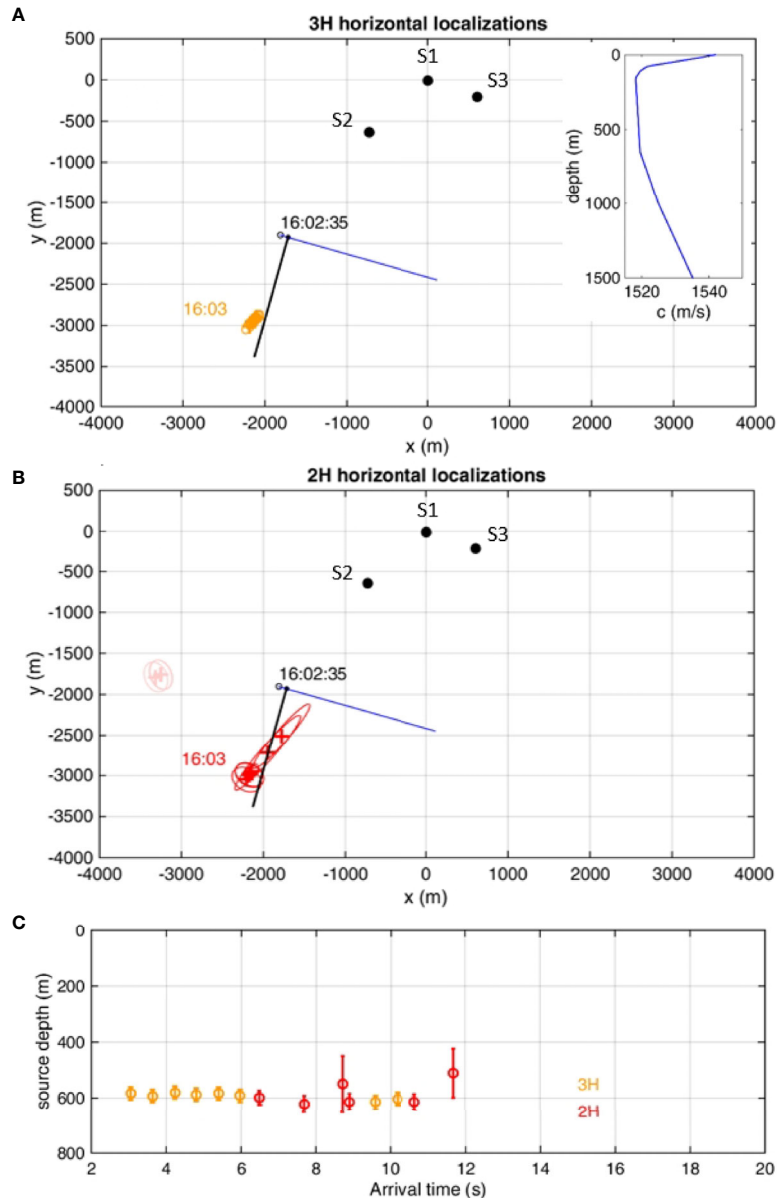


**FIGURE 10 | (A, B)** Localization results (in orange/red) on 16 July 2021 at 16:03 in the horizontal and **(C)** in the vertical based on receptions at three (3H) or two (2H) hydrophones. The symmetric solutions from 2H localization in the horizontal are also shown (light red) in **(B)**. The embedded graph in **(A)** shows the sound-speed profile measured in mid July. The blue line and the open circle in **(A, B)** show the vessel course and position, respectively, at 16:02:35; the black line shows the broadside direction of the towed array of hydrophones.

connecting the two hydrophones. In **Figure 10B** the symmetric solutions from the SWAN1-SWAN2 localizations are shown in light red; those from the other two hydrophone pairs (SWAN1-SWAN3 and SWAN2-SWAN3) are in shallow water and they are not shown. It is interesting to observe that the intersection of all 2H localizations defined by the corresponding uncertainty ellipses in **Figure 10B** results in an area that falls within the uncertainty ellipses of the 3H localizations of **Figure 10A**, and all are in agreement with the independent observations from the verification cruise.

The source depth estimates from all 14 localizations are shown in the lower panel in **Figure 10**. The source depth estimates from the 3H localizations are at about 600 m with uncertainties less than 30 m RMS. 2H localizations from SWAN1-SWAN2 and SWAN2-SWAN3 agree with these estimates and have similar uncertainties. In contrast, 2H localizations from SWAN1-SWAN3 result in large depth uncertainties, as in the case of range uncertainties in **Figure 10B**, because of the source being close to the broadside of the SWAN1-SWAN3 pair. Since the verification campaign

provided only bearing estimates there are no depth data to compare with.

As already mentioned, the above described processing stages are automatically performed for each 1-minute acoustic recording received at the analysis center. The intermediate results were presented here as a showcase demonstration. In the following only the final localization results for cases “B” and “C” are presented.

#### 4.1.2 Case “B” (16 July 2021 16:12:41)

The nearest localization in this case is from the recording starting at 16:12 and it is based on 2 hydrophones, SWAN1 and SWAN2. The results are presented (in red) in **Figure 11** where the top panel shows the localization in the horizontal and the course and location of the vessel at 16:12:41 (blue line and black circle respectively). The black line perpendicular to the course 100 m behind the vessel indicates the broadside direction. The localizations (in red) are consistent with each other. They lag the broadside line by about 250m and have a distance from the vessel course of about 250 m, much smaller than that in case “A”. On the other hand, the symmetric solutions, shown in light red, are more than 2 km away. The depth estimates are all at about the same depth, 700 m, with comparable and consistent uncertainties, about 30 m RMS, as shown in the lower panel of **Figure 11**.

#### 4.1.3 Case “C” (21 July 2021 17:25:26)

The localization in this case is based again on 2 hydrophones, SWAN1 and SWAN2. The top panel of **Figure 12** shows the localization results in the horizontal (in red) from the receptions at 17:27 which is closest to the observation time. It also shows the course and location of the vessel at 17:25:26 (blue line and black circle respectively) and the broadside direction marked by the black line perpendicular to the course 100 m behind the vessel. The localizations are in good agreement with the independent observations, whereas the symmetric solutions, shown in light red, are again more than 2 km away. The source here is in about the same azimuthal direction with respect to the acoustic stations as in case “B” but at larger distance (4.7 km from SWAN1) – note the different scales. Because of this the localization uncertainties are higher. The localization results in the vertical are shown in the lower panel of **Figure 12** with estimated source depths about 700 m and uncertainties of about 40 m RMS.

### 4.2 A Sperm-Whale Trajectory

In the early hours of 21 July 2021 a series of subsequent localizations between 3:36 and 6:18 resulted in a nice sperm-whale trajectory as shown in **Figure 13**. In this figure 3D localization results are shown, with the estimated depth represented by the color scale. The clear trajectory in the absence of any other localizations for a period of about 3

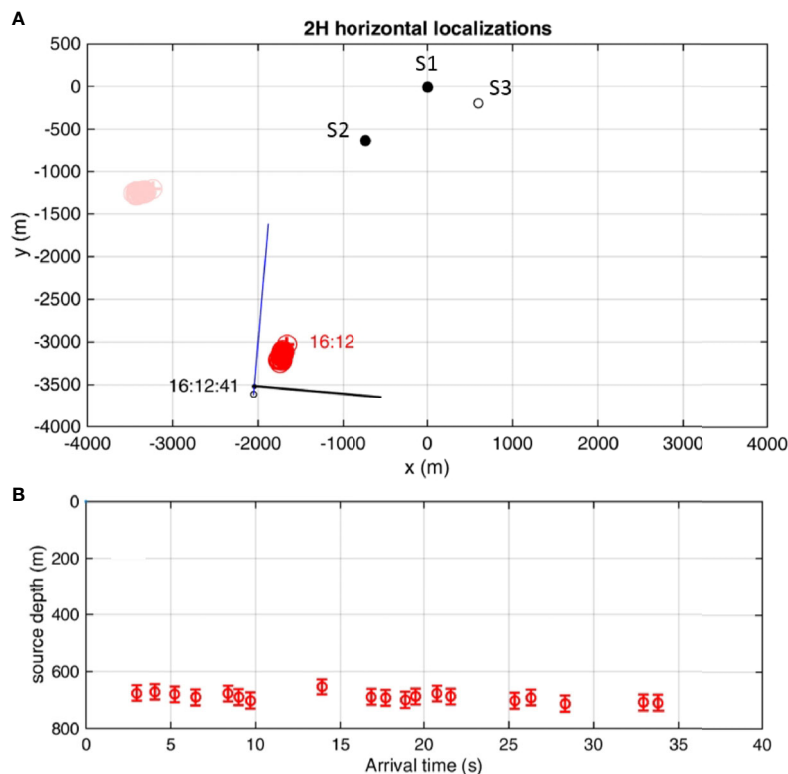


**FIGURE 11** | Localization results (in red) on 16 July 2021 at 16:12 (A) in the horizontal and (B) in the vertical based on receptions at SWAN1 and SWAN2 hydrophones. The symmetric solutions in the horizontal are also shown (light red) in (A). The blue line and the open circle in (A) show the vessel course and position, respectively, at 16:12:41; the black line shows the broadside direction of the towed array of hydrophones.

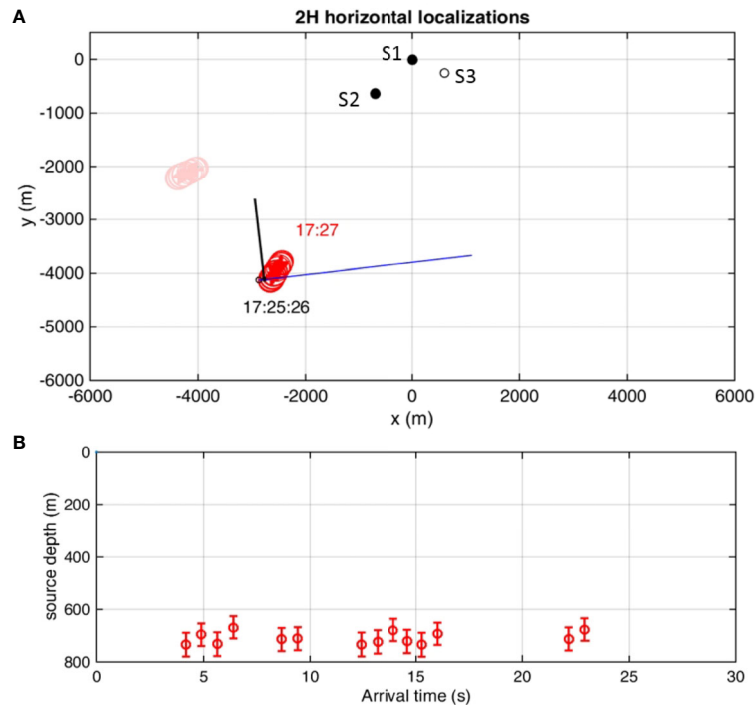


**FIGURE 12** | Localization results (in red) on 21 July 2021 at 17:27 **(A)** in the horizontal and **(B)** in the vertical based on receptions at SWAN1 and SWAN2 hydrophones. The symmetric solutions in the horizontal are also shown (light red) in **(A)**. The blue line and the open circle in **(A)** show the vessel course and position, respectively, at 17:25:26; the black line shows the broadside direction of the towed array of hydrophones.

hours suggests that this was probably a solitary mature male sperm whale. The trajectory spans a distance of about 10 km at distances between 2 and 6 km from the SWAN moorings and describes a course from east to west roughly along the 1000-m isobath. Although the localization uncertainties increase with distance from the observatory, they are still small enough to describe a meaningful trail.

The first localization occurred at 3:36 at a depth of 900 m and range of 6 km to the southeast from SWAN1, the central station. The subsequent localizations indicated a motion path to the northwest with depths changing between 750 and 950 m. At 4:12 a last localization at a depth of 650-700 m was carried out, pointing to an ascending animal. The next localization came 21 minutes later at 4:33. This time period fits well to an ascending

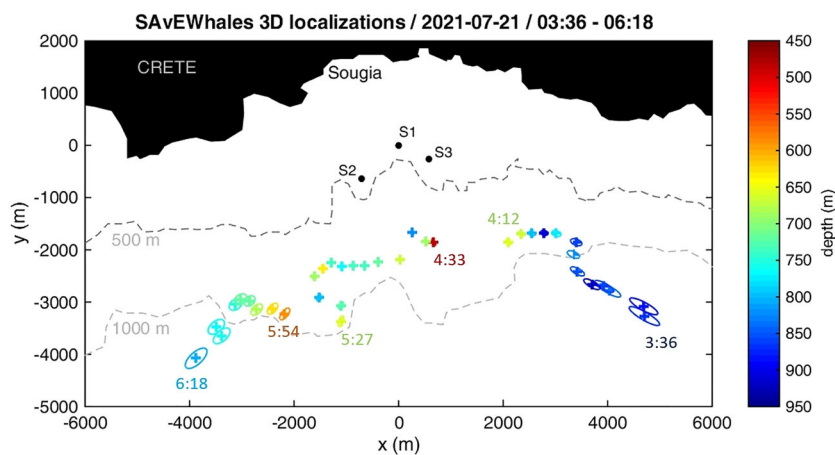


**FIGURE 13** | Localization results in the horizontal and in the vertical (color scale) in the early hours of 21 July 2021, between 03:36 and 06:18, defining a 3D sperm whale trajectory. A short video of this trajectory is also provided as supplementary material.

silent period of about 8 min, a surfacing period of about 10 min and a silent descending period (after the fluking) of about two minutes. These are typical times for the non-'regularly clicking phases' of the dive cycle of sperm whales that have been recorded in the area for many years.

The localization at 4:33 is at a depth of 450-500 m and fittingly displaced to the west compared to the previous one. The subsequent localizations indicate increasing depths up to 800 m followed by shallower depths about 750 m. The last localization of this dive cycle is at 5:27 at a depth of 650-700 m, pointing to a second ascend to the surface. The time period between the first and last localization of this dive cycle is 54 min, consistent with diving durations for mature male sperm whales (Amano and Yoshioka, 2003; Watwood et al., 2006). The first localization in the third dive cycle comes 27 min later at 5:54 at a depth of 550-600 m about 1 km to the west of the previous localization. Subsequent localizations show an increase in depth up to about 800 m up to the exit from the operation range of the system.

A time evolution view of the above localization sequence can be seen in the video file, which is provided as **Supplementary Material**.

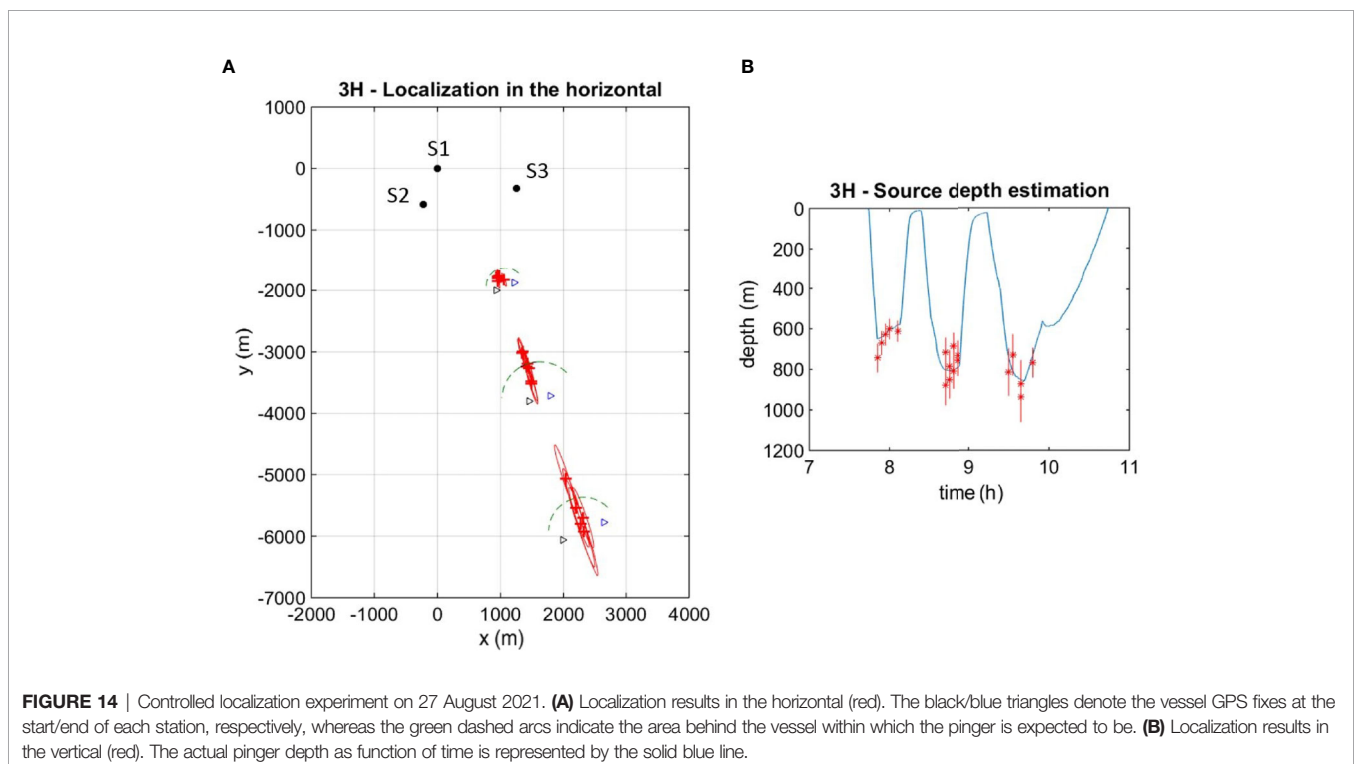
### 4.3 Results from the Controlled Localization Experiment

On 27 August 2021 between 7:00 and 11:00 a controlled localization experiment was conducted, as described in Section 3.3. **Figure 14** summarizes the results from this experiment. The three clusters of information in **Figure 14A** correspond to the three stations performed at increasing distances from the observatory (three black dots at the top). The GPS fixes at the start and at the end of each station (black and blue triangles,

respectively) indicated that there was a constant east-northeast drift during all stations due to wind and local currents.

The first station was performed at a distance of about 2 km south-southeast from the central mooring (SWAN1) and the pinger was lowered with a cable length of 700 m. The pinger reached a depth of about 650 m as it is seen from **Figure 14B** showing the actual pinger depth versus time (blue line). Because of the vessel drift, the pinger ascended to a depth of less than 600 m during the course of the station. Then the vessel moved to a location about 4 km from SWAN1 stopping for a second station where additional cable length was released to a total of 950 m. It is seen that during the tow from the first to the second station the pinger ascended nearly to the sea surface and then it sank to a depth of about 800 m. Finally the vessel moved 6 km away from SWAN1 to stop for a third station during which the pinger reached a depth of about 850 m. An approximate area behind the vessel within which the pinger is located can be estimated from the pinger depth and the cable length; the limits of this area are marked by green dashed arcs in **Figure 14A** for each station.

The localization results, marked in red, are in agreement with the actual pinger locations in both the horizontal and vertical direction. In the horizontal, the azimuth location of the pinger is accurately recovered and the ranges are in good agreement with the independent location estimates. The uncertainty ellipses are increasing with range in the radial direction meaning that the range uncertainties are higher for longer distances. On the other hand, the azimuth uncertainty remains nearly the same at all ranges, which is in agreement with theory (Pavlidis and Skarsoulis, 2021). Regarding localization in the vertical, the actual pinger depths are well recovered by the depth estimates



at all three stations (red dots and error bars in **Figure 14B**). The uncertainties of the depth estimates increase with distance – higher uncertainties at the third station compared to the first one –, similar to the behavior of the range uncertainties. The above results affirm the degree of localization accuracy provided by the SAvEWhales observatory.

## 5 DISCUSSION AND CONCLUSIONS

The development, deployment and operation of the SAvEWhales observatory for two 3-month periods in summer 2020 and 2021 demonstrated the feasibility of real-time monitoring of vocalizing sperm whales during their feeding dives. This can be a significant tool towards mitigation of ship strikes (collisions of animals with large ships), which is the most important threat for sperm whales in the Eastern Mediterranean Sea, particularly in cases where the major shipping lanes cross the Hellenic Trench and cannot be separated from the sperm whale habitats by a simple displacement.

By combining the real-time localization results with real-time ship-traffic data (Zissis et al., 2016; Frantzis et al., 2019) vessels at high collision risk in the broader area can be identified and notified for a suggested course change in an effort to avoid potential encounters. Given that the ascent period between the last click during a foraging dive and the surfacing of a whale is typically 6-11 minutes (Amano and Yoshioka, 2003; Watwood et al., 2006), a real-time localization based even on the last clicks of a dive cycle, allows for a considerable time margin for the conduct of avoidance maneuvers.

The SAvEWhales observatory proved effective in detecting and localizing sperm whales, particularly in summer 2021 where a large number of animals visited the deployment area, also during the period where a verification campaign was conducted. The large separation between the SAvEWhales buoys resulted in high localization accuracy, i.e. small localization uncertainties, associated with the large receiving aperture. At the same time this raised a number of challenges related mainly to synchronization and peak association between the buoys, as well as to partial data receptions – receptions not from all three hydrophones – due to directionality of sperm whale clicks. The synchronization issue was resolved by exploiting the PPS signals in the GPS receptions, and the peak association problem was addressed by applying a cross-correlation approach combined with geometric constraints. To address the problem of partial data receptions, the SAvEWhales system was designed to support both two- and three-hydrophone localization and select the most appropriate approach depending on the available data; in this connection, two-hydrophone localization proved to be a useful fallback option of the three-hydrophone array.

Further challenges arise in the case of social units, when several animals may be diving and producing regular clicks in the same area and at the same time; the question then is how to distinguish the different individuals in the localization analysis. A first indication of such a situation is the existence of more than one significant peaks in the TDOA histograms between direct

and surface-reflected arrivals corresponding to different source range/depth combinations. The ICIs of the corresponding arrivals at the different hydrophones, if different, can also be used to distinguish between different animals. In most receptions during system operation, a single ICI was matched at all three hydrophones, nevertheless there were a few recordings where two ICIs could be matched and helped distinguish between nearby individuals. The development of robust TDOA/ICI-based filtering methods for the localization of simultaneously clicking animals is currently work in progress.

Another important issue to be investigated is the optimal depth for hydrophone placement. SAvEWhales localizations rely on the resolution of direct and surface-reflected arrivals at each hydrophone. Given that the TDOA between direct and surface-reflected arrivals decreases as the source distance increases, there is a range limitation on localization applicability. For hydrophone depths of about 100 m and whale depths above 500-600 m the resolution limit between direct and surface-reflected arrivals is reached at distances of 6-7 km, depending on sound propagation conditions, which means that 3D localizations can be achieved up to that range.

By increasing the hydrophone depths, the time difference between direct and surface-reflected arrivals will increase as well resulting in an increase in the ranges over which direct and surface-reflected arrivals can be resolved. On the other hand, refraction can give rise to multipath and overlapping arrivals at longer ranges, which in turn will hamper the analysis (Mathias et al., 2013; Pavlidi and Skarsoulis, 2021). Thus, the optimal hydrophone depth, enabling localizations at maximum possible ranges, depends on the propagation conditions in the specific deployment area and should result from a study of the multipath behavior and resolvability between direct and surface-reflected arrivals on a case-by-case basis.

As already mentioned, the sound-speed profiles used for the localizations in the 2020 and 2021 deployments were obtained from regular *in situ* temperature measurements during maintenance visits. An independent temperature-profiling instrument using a thermistor chain for automatic updating of the sound-velocity profile was initially designed, yet not implemented since the sound-speed changes over the 3-month deployment periods were efficiently described by the almost biweekly *in situ* visits and measurements. For longer-term deployments an automatic sound-speed updating mechanism based on routine temperature profile measurements would be useful.

Even though the acoustic stations were initially designed for operation in calm weather conditions, assuming low to moderate wave forcing and mild currents, the actual conditions encountered in the field were much worse. In fall 2020, in the aftermath of a strong hurricane, extreme currents set in and sank two of the buoys. In summer 2021 extreme weather conditions were encountered as well, nevertheless the new buoys with increased excess buoyancy survived these situations, albeit with increased wearing in the anchor lines and anchor drag (even though the anchor and chain weights were doubled in 2021). For a longer-term operation of the SAvEWhales observatory a careful study and redesign of the mooring and anchoring system would be

necessary. Furthermore, energy consumption and storage capacity has to be reconsidered, to allow for operation in limited solar power conditions such as in winter period and/or higher latitudes. Alternatively, the solution of a cabled observatory, which would solve most of these problems, should be considered.

## DATA AVAILABILITY STATEMENT

The article contains first results from the SAvEWales project. The raw data remain with the authors for further analyses. Inquiries can be directed to the corresponding author.

## ETHICS STATEMENT

Ethical review and approval was not required for the animal study because the system presented was entirely passive (listening only) and remotely detected/localized sperm whales from their vocalizations. Therefore, it did not interact with the animals at all in any way. Visual observations of the whales where also conducted from safe distance and without any interaction with the animals under permit by the Greek Ministry of Environment.

## AUTHOR CONTRIBUTIONS

The development of the acoustic observatory was coordinated by ES, who was also in charge of the detection and localization methodology and the detailed analysis. GP was responsible for the development and assembly of the acoustic stations, as well as for their maintenance in the field, and he also participated in the detailed analysis. EO was in charge of the software on board the acoustic stations, as well as at the data reception and analysis center. PP contributed to the assembly of the acoustic stations as well as to field work. DP contributed to the development of the 3H localization method. MK contributed to the development of

data formats as well as to dissemination. PA contributed in the organization of the verification cruises and the analysis of the data collected. AF coordinated the SAvEWales project and was in charge of the verification cruises. All authors contributed to the article and approved the submitted version.

## FUNDING

This work was supported by OceanCare (Switzerland), who funded the SAvEWales (System for the Avoidance of Ship-Strikes with Endangered Whales) project.

## ACKNOWLEDGMENTS

For the deployment of the SAvEWales observatory in the Bay of Sougia special permits were granted by the Greek authorities. The authors would like to thank the crew of FV ELENA, Stelios Gialinakis in particular, as well as Michalis Pirovolakis and Giannis Paterakis from Sougia, and the officers of the port authority of Paleochora for their assistance. Further, they would like to thank the participants of the verification campaign, captain Radamanthys Fountoulakis, the research assistant Vangelis Moschopoulos and the eco-volunteers Eva Papadogianni, Stavroula Prasanaki, Fragkiski Panagou, Kalliopi Mpalourdou, Ermis Alexiadis and Aggeliki Papanikita for their contribution to the validation field work. We are grateful to OceanCare (Switzerland) for funding the SAvEWales project and supporting sperm-whale research and conservation in Greece since 2008.

## SUPPLEMENTARY MATERIAL

The Supplementary Material for this article can be found online at: <https://www.frontiersin.org/articles/10.3389/fmars.2022.873888/full#supplementary-material>

## REFERENCES

- Amano, M., and Yoshioka, M. (2003). Sperm Whale Diving Behavior Monitored Using a Suction-Cup-Attached TDR Tag. *Mar. Ecol. Progr. Ser.* 258, 291–295. doi: 10.3354/meps258291
- Angelier, J., Lyberis, N., Le Pichon, X., Barrier, E., and Huchon, P. (1982). The Tectonic Development of the Hellenic Arc and the Sea of Crete: A Synthesis. *Tectonophysics* 86, 159–196. doi: 10.1016/0040-1951(82)90066-X
- Baggenstoss, P. M. (2011). An Algorithm for the Localization of Multiple Interfering Sperm Whales Using Multi-Sensor Time Difference of Arrival. *J. Acoust. Soc. Am.* 130, 102–112. doi: 10.1121/1.3598454
- Barlow, J., Fregosi, S., Thomas, L., Harris, D., and Griffiths, E. T. (2021). Acoustic Detection Range and Population Density of Cuvier's Beaked Whales Estimated From Near-Surface Hydrophones. *J. Acoust. Soc. Am.* 149, 111–125. doi: 10.1121/10.0002881
- Barlow, J., Griffiths, E. T., Klinck, H., and Harris, D. V. (2018). Diving Behavior of Cuvier's Beaked Whales Inferred From Three-Dimensional Acoustic Localization and Tracking Using a Nested Array of Drifting Hydrophone Recorders. *J. Acoust. Soc. Am.* 144, 2030–2041. doi: 10.1121/1.5055216
- Brunoldi, M., Bozzini, G., Casale, A., Corvisiero, P., Grosso, D., Magnoli, N., et al. (2016). A Permanent Automated Real-Time Passive Acoustic Monitoring System for Bottlenose Dolphin Conservation in the Mediterranean Sea. *PLoS One* 11, 1–35. doi: 10.1371/journal.pone.0145362
- Chen, C.-T., and Millero, F. J. (1977). Speed of Sound in Seawater at High Pressures. *J. Acoust. Soc. Am.* 62, 1129–1135. doi: 10.1121/1.381646
- Frantzis, A., Alexiadou, P., and Gkikopoulou, K. C. (2014). Sperm Whale Occurrence, Site Fidelity and Population Structure Along the Hellenic Trench (Greece, Mediterranean Sea). *Aquat. Conserv. Mar. Freshw. Ecosyst.* 24, 3–102. doi: 10.1002/aqc.2435
- Frantzis, A., Leaper, R., Alexiadou, P., Prospathopoulos, A., and Lekkas, D. (2019). Shipping Routes Through Core Habitat of Endangered Sperm Whales Along the Hellenic Trench, Greece: Can We Reduce Collision Risks? *PLoS One* 14 (2), e0212016. doi: 10.1371/journal.pone.0212016
- Gassmann, M., Henderson, E., Wiggins, S. M., Roch, M. A., and Hildebrand, J. A. (2013). Offshore Killer Whale Tracking Using Multiple Hydrophone Arrays. *J. Acoust. Soc. Am.* 134, 3513–3521. doi: 10.1121/1.4824162
- Gassmann, M., Wiggins, S. M., and Hildebrand, J. A. (2015). Three-Dimensional Tracking of Cuvier's Beaked Whales' Echolocation Sounds Using Nested Hydrophone Arrays. *J. Acoust. Soc. Am.* 138, 2483–2494. doi: 10.1121/1.4927417
- Goold, J. C., and Jones, S. E. (1995). Time and Frequency-Domain Characteristics of Sperm Whale Clicks. *J. Acoust. Soc. Am.* 98, 1279–1291. doi: 10.1121/1.413465

- Grodsky, S. A., Reul, N., Bentamy, A., Vandemark, D., and Guimard, S. (2019). Eastern Mediterranean Salinification Observed in Satellite Salinity From SMAP Mission. *J. Mar. Syst.* 198, 103190. doi: 10.1016/j.jmarsys.2019.103190
- Hastie, G. D., Swift, R. J., Gordon, J. C. D., Slessor, G., and Turrell, W. R. (2003). Sperm Whale Distribution and Seasonal Density in the Faroe Shetland Channel. *J. Cetacean Res. Manage.* 5, 247–252.
- IUCN, International Union for the Conservation of Nature – Marine Mammal Protected Areas Task Force (2017). “First IMMA Regional Workshop for the Mediterranean, Chania, Greece, 24–28 October 2016,” in *Workshop Report*. Available at: <https://www.marinemammalhabitat.org/download/final-report-regional-workshop-mediterranean-sea-important-marine-mammal-areas/>.
- Jaquet, N., Dawson, S., and Douglas, L. (2001). Vocal Behavior of Male Sperm Whales: Why do They Click? *J. Acoust. Soc. Am.* 109, 2254–2259. doi: 10.1121/1.1360718
- Leaper, R., Chappell, O., and Gordon, J. C. D. (1992). The Development of Practical Techniques for Surveying Sperm Whale Populations Acoustically. *R. Int. Whal. Commun.* 42, 42549–42560.
- Le Pichon, X., and Angelier, J. (1979). The Hellenic Arc and Trench System: A Key to the Evolution of the Eastern Mediterranean Area. *Tectonophysics* 60, 1–42. doi: 10.1016/0040-1951(79)90131-8
- Lewis, T., Boisseau, O., Danbolt, M., Gillespie, D., Lacey, C., Leaper, R., et al. (2018). Abundance Estimates for Sperm Whales in the Mediterranean Sea From Acoustic Line-Transsect Surveys. *J. Cetac. Res. Manage.* 18, 103–117.
- Madsen, P. T., Payne, R., Kristiansen, N. U., Wahlberg, M., Kerr, I., and Møhl, B. (2002). Sperm Whale Sound Production Studied With Ultrasound Time/Depth-Recording Tags. *J. Exp. Biol.* 205, 1899–1906. doi: 10.1242/jeb.205.13.1899
- Marino, L. (2004). Cetacean Brain Evolution Multiplication Generates Complexity. *Int. J. Comp. Psychol.* 17, 3–4.
- Mathias, D., Thode, A. M., Straley, J., and Andrews, R. D. (2013). Acoustic Tracking of Sperm Whales in the Gulf of Alaska Using a Two-Element Vertical Array and Tags. *J. Acoust. Soc. Am.* 134, 2446–2461. doi: 10.1121/1.4816565
- McClain, C. R., Balk, M. A., Benfield, M. C., Branch, T. A., Chen, C., Cosgrove, J., et al. (2015). Sizing Ocean Giants: Patterns of Intraspecific Size Variation in Marine Megafauna. *PeerJ* 3, e715. doi: 10.7717/peerj.715
- Miller, B., and Dawson, S. (2009). A Large-Aperture Low-Cost Hydrophone Array for Tracking Whales From Small Boats. *J. Acoust. Soc. Am.* 126, 2248–2256. doi: 10.1121/1.3238258
- Miller, B., Dawson, S., and Vennell, R. (2013). Underwater Behavior of Sperm Whales Off Kaikoura, New Zealand, as Revealed by a Three-Dimensional Hydrophone Array. *J. Acoust. Soc. Am.* 134, 2690–2700. doi: 10.1121/1.4818896
- Morrissey, R., Ward, J., DiMarzio, N., Jarvis, S., and Moretti, D. J. (2006). Passive Acoustic Detection and Localization of Sperm Whales (Physeter Macrocephalus) in the Tongue of the Ocean. *Appl. Acoust.* 67, 1091–1105. doi: 10.1016/j.apacoust.2006.05.014
- Notarbartolo di Sciarra, G., Frantzis, A., Bearzi, G., and Reeves, R. R. (2006). “Sperm Whale Physeter Macrocephalus (Mediterranean Subpopulation),” in *The Status and Distribution of Cetaceans in the Black Sea and Mediterranean Sea* (Malaga: IUCN Centre for Mediterranean Cooperation).
- Park, I., Paiva, A. R. C., DeMarse, T. B., and Principe, J. C. (2008). An Efficient Algorithm for Continuous Time Cross Correlogram of Spike Trains. *J. Neurosci. Meth.* 168, 514–523. doi: 10.1016/j.jneumeth.2007.10.005
- Pavli, D., and Skarsoulis, E. K. (2021). Enhanced Pulsed-Source Localization With 3 Hydrophones: Uncertainty Estimates. *Rem. Sens.* 13 (9), 1817. doi: 10.3390/rs13091817
- Rideout, B. P., Dosso, S. E., and Hannay, D. E. (2013). Underwater Passive Acoustic Localization of Pacific Walruses in the Northeastern Chukchi Sea. *J. Acoust. Soc. Am.* 134, 2534–2545. doi: 10.1121/1.4816580
- Roth, G., and Dicke, U. (2005). Evolution of the Brain and Intelligence. *Trends Cogn. Sci.* 9, 250–257. doi: 10.1016/j.tics.2005.03.005
- Sanguineti, M., Alessi, J., Brunoldi, M., Cannarile, G., Cavalleri, O., Cerruti, R., et al. (2021). An Automated Passive Acoustic Monitoring System for Real Time Sperm Whale (Physeter Macrocephalus) Threat Prevention in the Mediterranean Sea. *Appl. Acoust.* 172. doi: 10.1016/j.apacoust.2020.107650
- Skarsoulis, E. K., and Dosso, S. E. (2015). Linearized Two-Hydrophone Localization of a Pulsed Acoustic Source in the Presence of Refraction: Theory and Simulations. *J. Acoust. Soc. Am.* 138, 2221–2234. doi: 10.1121/1.4930937
- Skarsoulis, E. K., Frantzis, A., and Kalogerakis, M. (2004). “Passive Localization of Pulsed Sound Sources With a 2-Hydrophone Array”, in Simons, Dick, G editor. *Proceedings of the Seventh European Conference on Underwater Acoustics (ECUA)*, 5–8 July (Delft, The Netherlands: Published by Delft University of Technology). Available at: <https://www.abebooks.com/PROCEEDINGS-SEVENTH-EUROPEAN-CONFERENCE-UNDERWATER-ACOUSTICS/11440284069/bd>.
- Skarsoulis, E. K., and Kalogerakis, M. A. (2005). Ray-Theoretic Localization of an Impulsive Source in a Stratified Ocean Using Two Hydrophones. *J. Acoust. Soc. Am.* 118, 2934–2943. doi: 10.1121/1.2041267
- Skarsoulis, E. K., and Kalogerakis, M. A. (2006). Two-Hydrophone Localization of a Click Source in the Presence of Refraction. *Appl. Acoust.* 67, 1202–1212. doi: 10.1016/j.apacoust.2006.05.009
- Skarsoulis, E. K., Piperakis, G., Kalogerakis, M., Orfanakis, E., Papadakis, P., Dosso, S. E., et al. (2018). Underwater Acoustic Pulsed Source Localization With a Pair of Hydrophones. *Remote Sens.* 10 (6), 883. doi: 10.3390/rs10060883
- Teloni, V. (2005). Patterns of Sound Production in Diving Sperm Whales in the Northwestern Mediterranean. *Mar. Mamm. Sci.* 21, 446–457. doi: 10.1111/j.1748-7692.2005.tb01243.x
- Thode, A. (2004). Tracking Sperm Whale (Physeter Macrocephalus) Dive Profiles Using a Towed Passive Acoustic Array. *J. Acoust. Soc. Am.* 116, 245–253. doi: 10.1121/1.1758972
- Thode, A. (2005). Three-Dimensional Passive Acoustic Tracking of Sperm Whales (Physeter Macrocephalus) in Ray-Refracting Environments. *J. Acoust. Soc. Am.* 118, 3575–3584. doi: 10.1121/1.2049068
- Tran, D. D., Huang, W., Bohn, A. C., Gong, Z., Makris, N. C., and Ratilal, P. (2014). Using a Coherent Hydrophone Array for Observing Sperm Whale Range, Classification, and Shallow-Water Dive Profiles. *J. Acoust. Soc. Am.* 135, 3352–3363. doi: 10.1121/1.4874601
- Urazghildiiev, I. R., and Hannay, D. (2017). Maximum Likelihood Estimators and Cramér–Rao Bound for Estimating Azimuth and Elevation Angles Using Compact Arrays. *J. Acoust. Soc. Am.* 141, 2548–2555. doi: 10.1121/1.4979792
- Urazghildiiev, I. R., and Hannay, D. E. (2020). Localizing Sources Using a Network of Asynchronous Compact Arrays. *IEEE J. Ocean. Eng.* 45, 1091–1098. doi: 10.1109/JOE.2019.2915913
- Wahlberg, M., Møhl, B., and Teglberg, M. P. (2001). Estimating Source Position Accuracy of a Large-Aperture Hydrophone Array for Bioacoustics. *J. Acoust. Soc. Am.* 109, 397–406. doi: 10.1121/1.1329619
- Watkins, W. A., Daher, M. A., Frstrup, K. M., and Howald, T. (1993). Sperm Whales Tagged With Transponders and Tracked Underwater by Sonar. *Mar. Mammal Sci.* 9, 55–67. doi: 10.1111/j.1748-7692.1993.tb00426.x
- Watkins, W. A., and Schevill, W. E. (1972). Sound Source Location by Arrival-Times on a non-Rigid Three-Dimensional Hydrophone Array. *Deep Sea Res. Oceanogr. Abstr.* 19, 691–706. doi: 10.1016/0011-7471(72)90061-7
- Watwood, S. L., Miller, P. J. O., Johnson, M., Madsen, P. T., and Tyack, P. L. (2006). Deep-Diving Foraging Behaviour of Sperm Whales (Physeter Macrocephalus). *J. Anim. Ecol.* 75, 814–825. doi: 10.1111/j.1365-2656.2006.01101.x
- Zimmer, W. M. X., Tyack, P. L., Johnson, M. P., and Madsen, P. T. (2005). Three-Dimensional Beam Pattern of Regular Sperm Whale Clicks Confirms Bent-Horn Hypothesis. *J. Acoust. Soc. Am.* 117, 1473–1485. doi: 10.1121/1.1828501
- Zissis, D., Xidias, E. K., and Lekkas, D. (2016). Real-Time Vessel Behavior Prediction. *Evolving Systems* 7, 29–40. doi: 10.1007/s12530-015-9133-5

**Conflict of Interest:** The authors declare that the research was conducted in the absence of any commercial or financial relationships that could be construed as a potential conflict of interest.

**Publisher’s Note:** All claims expressed in this article are solely those of the authors and do not necessarily represent those of their affiliated organizations, or those of the publisher, the editors and the reviewers. Any product that may be evaluated in this article, or claim that may be made by its manufacturer, is not guaranteed or endorsed by the publisher.

Copyright © 2022 Skarsoulis, Piperakis, Orfanakis, Papadakis, Pavli, Kalogerakis, Alexiadou and Frantzis. This is an open-access article distributed under the terms of the Creative Commons Attribution License (CC BY). The use, distribution or reproduction in other forums is permitted, provided the original author(s) and the copyright owner(s) are credited and that the original publication in this journal is cited, in accordance with accepted academic practice. No use, distribution or reproduction is permitted which does not comply with these terms.